MONOTONIC, MULTIDIMENSIONAL FLUX DISCRETIZATION SCHEME FOR ALL PECLET NUMBERS

Tony W. H. Sheu, S. F. Tsai, and S. K. Wang
Department of Naval Architecture and Ocean Engineering, National Taiwan University, Taipei, Taiwan, Republic of China

The focus of this work is to resolve discontinuities in the flow by a hybrid scheme comprising two classes of flux discretization schemes. Construction of a stiffness matrix having the M-matrix property is desirable in finite-element codes for capturing a solution profile with an appreciable gradient. In this study, two finite-element formulations capable of yielding an irreducible diagonal dominant type of matrix equation are proposed and compared. The first class of finite-element method is suited for high-Peclet-number problems and is formulated within the Galerkin context. The other class of upwind scheme, which is applicable to lower-Peclet-number flows, falls into the Petrov-Galerkin category. The finite-element test and basis spaces are spanned by Legendre polynomials. Assessment studies are made, with emphasis on the accuracy and stability of the solution. We also address the sensitivity of this scheme to Peclet numbers in obtaining monotonic solutions. Numerical investigation reveals that the proposed scheme is effective in producing monotonic solutions at high- and low-Peclet-number conditions.

INTRODUCTION

A computer code with good discontinuity-capturing capability is a challenging task to develop for simulating high-speed gas dynamics or incompressible hydrodynamics. Since the simplest prototype equation characterizing these flows is that of the scalar convection-diffusion equation, the flux discretization scheme for the solution of this passive transport equation is a subject of fundamental importance in fluid mechanics and has been the focus of many intensive studies over the last few decades. Working equations of this type are also of considerable engineering interest because they are amenable to analytic solution. Investigation of this equation is instructive for detailed assessment of the discretization methods so far devised. It is for these reasons that this model problem is the continuous subject of much research interest, academically as well as practically.

Over the last 40 years, considerable progress has been made in numerical modeling of the scalar convection-diffusion equation. There remain some notori-

Received 23 October 1996; accepted 2 January 1997.

The authors would like to thank the Computer Center of National Taiwan University and the National Center for High-Performance Computing (NCHC) for providing CRAY J916 and IBM RS/6000-590 computers, which made this study possible.

Address correspondence to Tony W. H. Sheu, Department of Naval Architecture and Ocean Engineering, National Taiwan University, 73 Chou-Shan Road, Taipei, Taiwan. E-mail: sheu@indy.na.ntu.edu.tw

Numerical Heat Transfer, Part B, 31:441–457, 1997

1040–7790/97 $12.00 + .00

NOMENCLATURE

h	mesh size	W_i	weighting function
h_ξ, h_η	mesh sizes in the computational plane	$\delta_{i,j}$	permutation notation
J	Jacobian of the transformation	$\Delta x, \Delta y$	mesh size along the x and y directions, respectively
N_i	basis test function		
P_i	ith term of the Legendre polynomial	μ	diffusivity of the fluid
Pe	Peclet number	ξ, η	normalized spatial coordinates
s	streamline coordinate	Φ	primary variable for the scalar transport equation
T	truncation error		
u, v	velocity component in x and y directions, respectively		

ous difficulties to be circumvented, and answers are not definite yet. Examples include, among other difficulties, numerical modeling of fluxes in a multidimensional region where convection prevails. In many cases, flow discontinuities in the flow may further complicate the analysis, due to the possible presence of wiggles in high-gradient regions. The need to suppress these oscillatory solutions motivated the present study. Flux discretization errors can be broadly divided into two main categories: those that deal mainly with dissipation and dispersion, and those that deal with numerical diffusion as a whole. Numerical dissipation refers to artificially introduced smearing of the predicted profile, while numerical dispersion refers to nonphysical spatial oscillations in the solution. Besides solution accuracy, numerical stability, and scheme consistency, an efficient numerical simulation also involves computational efficiency and ease of programming. These desired properties are, however, difficult to achieve simultaneously. What fits for solution accuracy may not for solution stability. The focus for this study is solution monotonicity and accuracy.

Numerical solutions to multidimensional flow equations are often grossly smeared by excessive addition of false diffusion errors. Employing a flow-oriented flux discretization scheme serves as a way to circumvent this deterioration of the solution. In many flows, steep gradients appear, causing the solution to deteriorate further. In these circumstances, a flow-oriented flux discretization scheme no longer suffices for production of oscillation-free solutions. Difficulties in suppressing over- or undershoots in the solution have led to the development of bounding schemes. Much of the previous work has been devoted to designing a scheme that can accommodate the total variational diminishing (TVD) property [1]. However, we encounter difficulty in extending the underlying criterion of the TVD conditions to multidimensional analyses.

The flux-corrected transport (FCT) algorithm of Boris and Book [2], which was later generalized by Zalesak [3], is regarded as the first multidimensional high-resolution scheme developed by the finite-difference/volume community. This scheme, together with the filter remedy and methodology (FARM) of Chapman [4] and other variants of flux limiters, have been applied to different classes of equations by one of the present authors [5, 6]. Among other schemes, the simple high-accuracy resolution program (SHARP) [7] and nonoscillatory, integrally reconstructed volume-averaged numerical advection (NIRVANA) scheme [8, 9],

developed by Leonard, and SMART (sharp and monotonic algorithm for realistic transport), developed by Gaskell and Lau [10], have also gained wide popularity. In a parallel development, the FCT algorithm has been applied to the Taylor-Galerkin framework to resolve sharp profiles [11–14]. The other approach for constructing oscillation-free schemes is to apply a global positivity principle to numerical analyses that were developed within the explicit context [15, 16]. While this principle has a sound basis in theory and is easy to implement in existing computer codes, its application scope is limited to explicit schemes. Filtering techniques, applicable to analyses that involve solving field variables from simultaneous algebraic equations, must be devised. To avoid erroneous oscillations near jumps, we have modified the test functions defined in the streamline upwind Petrov-Galerkin (SUPG) model by means of added nonlinearities [6]. With this nonlinear addition, the resulting stiffness matrix ensures satisfaction of either the total variational diminishing property [1] or the maximum principle [17–19]. Exploiting this principle yields a monotonic solution profile. Instead of modifying the test functions, Rice and Schnipke [16] and Hill and Baskharone [20] took a different approach in an attempt to achieve the same goal. Integral terms involving convection terms were evaluated along the local streamline, thus providing a monotonic solution profile.

Recently, Ahue and Telias [19] used an exponential-biased test function to construct an M-matrix. Their success has prompted us to propose a biased weighting function that is constructed in favor of the upstream field variable. Guided by this mathematically rigorous theory, we have successfully captured sharp gradients or discontinuities in the flow [21, 22]. The purpose of this study is to assess this Petrov-Galerkin formulation against the monotone streamline upwind model of Rice and Schnipke [16].

We begin by describing the target problem, known as the convection-diffusion equation. We bring the monotonicity-preserving property into the Petrov-Galerkin framework. Bearing in mind that simulation quality depends on accuracy and stability, we have carried out fundamental studies and discussed them here in detail. In order to validate the proposed flux discretization scheme, we will present a problem which has a closed-form solution for the scalar transport equation and is defined in a square cavity. Attention is directed to assessing the scheme performance.

MULTIDIMENSIONAL FLUX DISCRETIZATION SCHEME

The working equation considered here is that of the transport equation for the passive scalar Φ:

$$u\Phi_x + v\Phi_y = \mu(\Phi_{xx} + \Phi_{yy}) \tag{1}$$

We consider in this study a simple flow given by $\mathbf{u} = (u, v)$, where u and v are two constants. This simplification avoids difficulties in handling nonlinearities in the equation. For simplicity, this article is concerned with a constant diffusion coefficient μ in a simply connected domain D. Due to the elliptic nature of the partial differential equation (1), closed-form solutions demand that boundary values of $\hat{\Phi}$ be prescribed at the entire boundary of the physical domain D.

Finite-element solutions, $\hat{\Phi}$, to the transport equation (1) are obtained by demanding that $R = u\hat{\Phi}_x + v\hat{\Phi}_y - \mu(\hat{\Phi}_{xx} + \hat{\Phi}_{yy})$ be orthogonal to the weighting function. Solutions thus obtained can be viewed as a search for the weak solutions to Eq. (1). Depending on the relative ratio of the convection and diffusion effects, as measured by the maximum values of $\mathrm{Pe}_x = u\,\Delta x/\mu$ and $\mathrm{Pe}_y = v\,\Delta y/\mu$, different test spaces $\{W_i\}$ are chosen for computational reasons. Here, Δx and Δy denote mesh sizes along the x and y directions, respectively. Within the weighted residuals context, substitution of bilinear basis functions N_i for $\hat{\Phi} = \sum_{i=1}^{4} N_i(\xi, \eta)\Phi_i$ into the weighted residual statement, $\int_e WR\,d\Omega_e = 0$, yields a matrix equation for the element e. Upon assemblage of finite elements, the global coefficient matrix is thus formed. There remains selection of a test function to close the algebraic system. How the weighting functions are constructed is of pivotal importance and warrants further discussion.

For problems involving multiple dimensions, the first-order derivative terms in Eq. (1) present numerical difficulties. While use of upwind approximation of these terms circumvents notorious difficulties arising from the direction-dependent fluxes, questions remain as to whether or not bounded solutions can be unconditionally computed. According to Ahue and Telias [19], a stiffness matrix of the irreducible diagonal dominant type is a key to constructing an M-matrix, which is needed to assure monotonic solutions. Construction of an M-matrix equation [17–19] can be achieved in different ways. Two alternatives underlying different ideas are considered in this article.

Monotonic Scheme Constructed by Legendre Polynomials

The first step in achieving the convective stability property for the differential equation (1) is to weigh convective fluxes unequally in favor of the upwind side. For purposes of consistency, diffusive fluxes are also bias-weighted in the weak sense. In conditions where bilinear basis functions are used to approximate the scalar transport variable Φ, use of conventional upwind finite-element schemes presents difficulties because of the insufficient polynomial degree used in the basis function when performing integration by parts on the diffusive flux and the biased part of the test function which, as is usual, involves $\partial N_i/\partial x$ or $\partial N_i/\partial y$. This motivated us to choose the finite-element space which is spanned by infinitely differentiable functions. Sheu et al. [21, 22] demonstrated that use of exponential weighting functions offers not only convective stability, but also the Peclet-number-dependent monotonic property for scalar as well as incompressible Navier-Stokes equations. One disadvantage inherent in this model is that use of exponential functions for finite-element integration can produce prohibitively high computational costs. This deficiency motivated further refinement of this model with a view to improving computational efficiency. In an attempt to arrive at this goal, we have constructed a new Legendre-polynomial test space [23]:

$$W_i = D_i\left[d_{\xi_0}P_0(\xi) + d_{\xi_1}P_1(\xi)\right]\left[d_{\eta_0}P_0(\eta) + d_{\eta_1}P_1(\eta)\right] \tag{2}$$

where

$$D_i = \frac{1}{4}\exp\left(\frac{uh_\xi \xi_i}{2\mu}\right)\exp\left(\frac{vh_\eta \eta_i}{2\mu}\right)$$

$$W_\xi(\xi) = (1 + \xi_i \xi)\exp\left(-\frac{uh_\xi \xi}{2\mu}\right)$$

$$W_\eta(\eta) = (1 + \eta_i \eta)\exp\left(\frac{-vh_\eta \eta}{2\mu}\right)$$

$$d_{\xi_n} = \frac{2n+1}{2}\int_{-1}^{1} W_\xi(t)P_n(t)\,dt$$

$$d_{\eta_n} = \frac{2n+1}{2}\int_{-1}^{1} W_\eta(t)P_n(t)\,dt$$

In Eq. (2), h_ξ and h_η denote grid sizes. Equation (2) involves the Legendre polynomials $P_0(t) = 1$ and $P_1(t) = t$. It is worth noting that the gain in computational efficiency is attributable mainly to the orthogonal property inherent in the finite-element space spanned by Legendre polynomials:

$$\int_{-1}^{+1} P_i(t)P_j(t)\,dt = \frac{2}{2i+1}\delta_{i,j} \qquad (i \text{ is a dummy index}) \tag{3}$$

This mathematically appealing integral identity considerably reduces the CPU time. It is for this reason that we are prompted to rewrite the bilinear shape functions $N_i(\xi, \eta)$ in terms of Legendre polynomials as follows:

$$N_i(\xi, \eta) = \frac{1}{4}[P_0(\xi) + \xi_i P_1(\xi)][P_0(\eta) + \eta_i P_1(\eta)] \tag{4}$$

It is also important to address here that matrix equations resulting from the use of the Legendre-polynomial weighting functions are exactly identical to those obtained by employing our previously developed exponential weighting functions. For the justification of using this upwind finite-element model and the proof of the mathematical equivalence between the Legendre and exponential polynomial based schemes, the reader is referred to the work of Sheu et al. [23].

Characteristic Galerkin Finite-Element Approach

Depending on the physical nature of flux terms, we divide them into two groups and discretize them separately. We can rewrite the convective flux terms in terms of the streamline coordinate s as follows:

$$u\Phi_x + v\Phi_y = u_s\Phi_s \tag{5}$$

As for diffusive fluxes, they are more suited to formulation conducted in the Cartesian coordinate system and are approximated in a weak sense by employing a Galerkin approach.

According to Rice and Schnipke [16], we take $u_s\Phi_s$ as a constant value in each element. Following the standard weighted-residuals finite-element procedures, we can derive the following weak form:

$$u_s \frac{\partial \Phi}{\partial s} \int W dA - \mu \int W(\Phi_{xx} + \Phi_{yy})\, dA = 0 \tag{6}$$

where W is the weighting functions. For purposes of consistency, weighting functions are chosen as the basis functions. The rationale behind choosing the Galerkin formulation is to avoid dealing with diffusive fluxes in conditions when bilinear shape functions are chosen for use. According to Figure 1, which depicts the flow direction within an element, we approximate $\partial\phi/\partial s$ as $(1/\Delta s)(\Phi_{ij} - \Phi')$, where

$$\Phi' = \frac{1}{a+b}(b\Phi_1 + a\Phi_2) \tag{7a}$$

$$a = (x_2 - x_1) - (y_3 - y_2)\frac{u}{v} \tag{7b}$$

$$b = (y_3 - y_2)\frac{u}{v} \tag{7c}$$

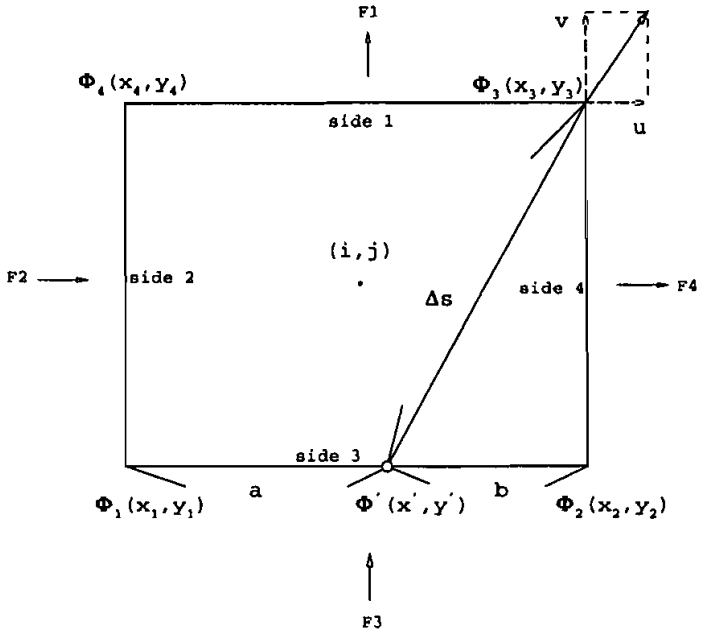

Figure 1. Illustrative plot showing the downwind node identification.

and

$$\Delta s = \left[(x_3 - x')^2 + (y_3 - y')^2\right]^{1/2} \tag{8}$$

It remains to determine the coordinates x', y', and the value of $\Phi(x', y')$. Take $u > 0$, $v > 0$ as an example. Incorporation of the characteristics into the Galerkin formulation is done by approximating $\Phi(x = x', y = y')$ as follows [16]:

$$\Phi' = (1 - F_p)\Phi_4 + (1 - F_n)\Phi_2 + F_p F_n \Phi_1 \tag{9}$$

where

$$0 \leqslant F_p \equiv \max\left\{\min\left(\frac{F_1}{F_2}, 1\right), 0\right\} \leqslant 1 \tag{10a}$$

$$0 \leqslant F_n \equiv \max\left\{\min\left(\frac{F_4}{F_3}, 1\right), 0\right\} \leqslant 1 \tag{10b}$$

Here, $F_i (i = 1\text{–}4)$ denote the outward normal facial fluxes:

$$F_1 = v(x_3 - x_4) + u(y_4 - y_3) \tag{11a}$$

$$F_2 = v(x_1 - x_4) + u(y_4 - y_1) \tag{11b}$$

$$F_3 = v(x_2 - x_1) + u(y_1 - y_2) \tag{11c}$$

$$F_4 = v(x_2 - x_3) + u(y_3 - y_2) \tag{11d}$$

The spatial location (x', y') is chosen as the extension of the velocity vector from the node (x_3, y_3) shown in Figure 1. Their coordinates are approximated by similar linear summation as those of Φ' defined in Eq. (9). By substituting Eqs. (7)–(11) into the Galerkin statement, as shown in Eq. (6), we can derive the following stiffness matrix for an element:

$$\begin{pmatrix} 0 & 0 & 0 & 0 \\ 0 & 0 & 0 & 0 \\ -F_p F_n \dfrac{u_s}{\Delta s} A_f & -(1 - F_n)\dfrac{u_s}{\Delta s} A_f & \dfrac{u_s}{\Delta s} A_f & -(1 - F_p)\dfrac{u_s}{\Delta s} A_f \\ 0 & 0 & 0 & 0 \end{pmatrix} \tag{12}$$

where

$$A_f = \iint N_3(\xi, \eta)|J|\, d\xi\, d\eta \tag{13}$$

FUNDAMENTAL STUDIES ON THE PROPOSED UPWIND MODEL

There are several areas that warrant detailed investigation before a newly developed discretization scheme can come into widespread use for industrial flows. Typical of them are accuracy and stability studies.

Following the standard procedures of Warming and Hyett [15], we can derive the following modified equation for our finite-element model:

$$u\Phi_x + v\Phi_y - \mu(\Phi_{xx} + \Phi_{yy}) = T \tag{14}$$

where

$$T = c_1\Phi_{xx} + c_2\Phi_{xy} + c_3\Phi_{yy} + d_1\Phi_{xxx} + d_2\Phi_{yyy} + d_3\Phi_{xxy} + d_4\Phi_{xyy} + e_1\Phi_{xxxx} + e_2\Phi_{xxxy} + e_3\Phi_{xxyy} + e_4\Phi_{xyyy} + e_5\Phi_{yyyy} + \cdots \tag{15}$$

Algebraic complications preclude functional expression of the coefficients shown in (15). To compensate for this, we express these coefficients numerically. According to Figure 2, the rates of convergence for Φ_{xxxy} and Φ_{xyyy} are $O(h^4)$, while those for Φ_{xy}, Φ_{xxx}, Φ_{yyy}, Φ_{xxy}, Φ_{xyy}, Φ_{xxxx}, Φ_{yyyy}, and Φ_{xxyy} are in the vicinity of $O(h^2)$. As for the leading terms, Φ_{xx} and Φ_{yy}, their errors are reduced by a convergence rate of $O(h^2)$. In light of these results, this fundamental analysis gives insight into the order of accuracy for the finite-element approximation constructed by using Legendre polynomials and helps to assure that a uniformly consistent property can be obtained.

According to Ahue and Telias [19], a monotonic prediction of the solution profile for Eq. (1) demands that the stiffness matrix be a real, irreducible, diagonally dominant matrix where off-diagonal entries are non-negative. At this point, it is instructive to examine whether the upwind scheme formulated on the basis of Legendre-polynomial finite-element spaces can be applied to yield an unconditionally monotonic solution. To this end, we derive the discrete finite-element equation with its coefficients expressed in terms of Peclet numbers. By varying the values of Pe_x and Pe_y, we compute the coefficients, from which we can determine whether or not it is possible to obtain the sufficient (but not necessary) condition of yielding a monotonic solution. In Figure 3, shown in the shaded area are the solutions computed under grid sizes for a given set of diffusivity and convective velocities, which are, by definition, monotonic.

NUMERICAL RESULTS

For purposes of validation, we consider first an analytic test problem. This problem is designed specifically to benchmark the solution accuracy and examine the solution monotonicity for two investigated upwind finite-element schemes. The question of whether the upwind schemes under investigation accommodate good discontinuity-capturing capability is answered by solving the well-known skew advection-diffusion problem.

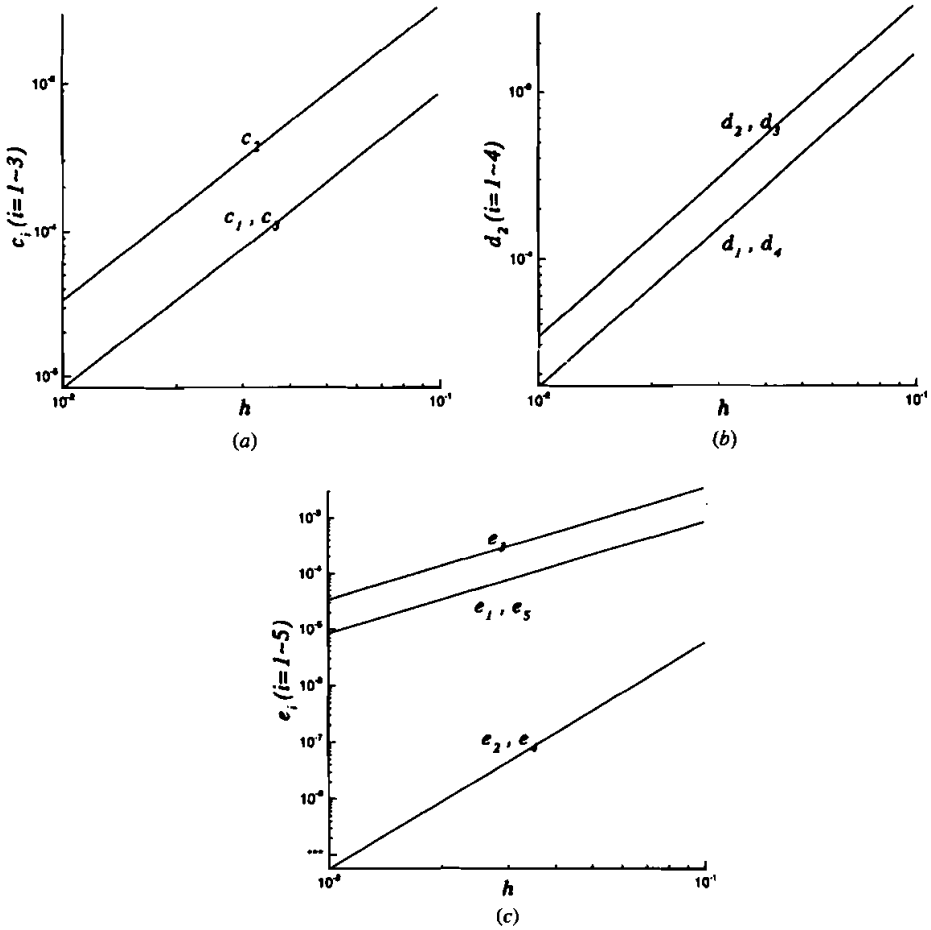

Figure 2. Computed rates of coefficients in Eq. (15): (*a*) $\Phi_{xx}, \Phi_{xy}, \Phi_{yy}$; (*b*) $\Phi_{xxx}, \Phi_{xxy}, \Phi_{xyy}, \Phi_{yyy}$; (*c*) $\Phi_{xxxx}, \Phi_{xxxy}, \Phi_{xxyy}, \Phi_{xyyy}, \Phi_{yyyy}$.

Analytic Study

The first problem we will deal with is configured in Figure 4. Subject to the analytically prescribed boundary data, the advection-diffusion equation (1) is amenable to a boundary-layer-type analytic solution:

$$\Phi(x, y) = \frac{\{1 - \exp[(x - 1)(u/\mu)]\}\{1 - \exp[(y - 1)(v/\mu)]\}}{[1 - \exp(-u/\mu)][1 - \exp(-v/\mu)]} \tag{16}$$

Finite-element solutions are sought in a square of unit length, that is covered with a uniform grid. We start from a very coarse grid, namely, 11 × 11, and proceed to continuously refined grids 21 × 21, 31 × 31, 41 × 41, and 51 × 51. For this study, numerical errors are computed and cast in the L_2 *norm* sense. We have

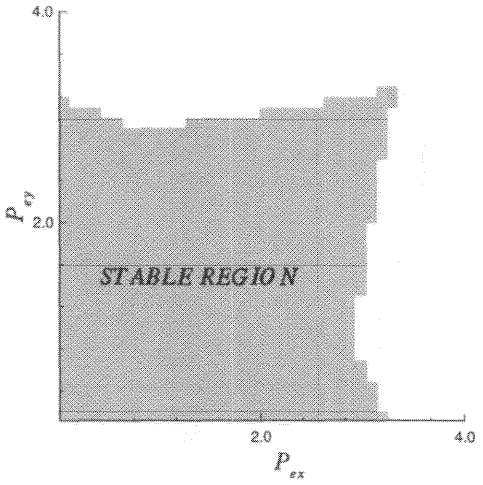

Figure 3. Illustration of the monotonic region underlying the proposed upwind scheme ($P_{ex} = \mathrm{Pe}_x$, $P_{ey} = \mathrm{Pe}_y$).

tabulized the L_2 *error* norms for the investigated schemes in Tables 1 and 2. As Table 1 reveals, the computed errors are due mainly to the machine errors. As to the computed errors shown in Table 2, they are continuously reduced with an increase of the grid density. It is thus instructive to plot $c = \log(\mathrm{err}_1/\mathrm{err}_2)/\log(M_2/M_1)$, from which the rates of convergence for both schemes can be clearly seen. Here, $\mathrm{err}_i (i = 1, 2)$ denotes L_2 norms of errors computed at two continuously refined grids, $(M_1 + 1)^2$ and $(M_2 + 1)^2$. Notably, computed solutions, as shown in Table 1, are highly accurate for $\mu = 1.0$, 0.1, and 0.01, so that the rates of convergence are meaningless. According to Table 2, the rates of convergence are plotted in Figure 5. Up to now, we can conclude that in pursuit of a high-resolution monotonic solution, it is preferable to apply the Legendre-polynomial finite-element model to problems with lower Peclet numbers and to apply

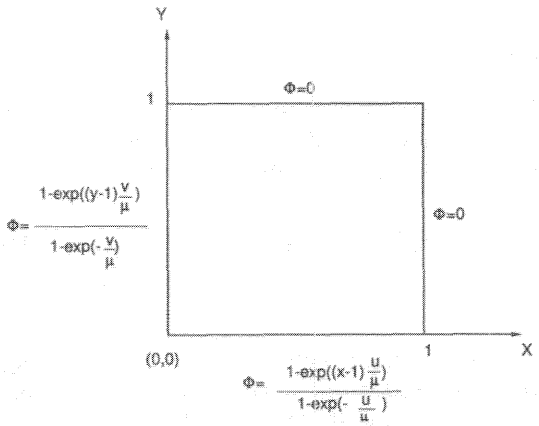

Figure 4. Illustration of the analytic test problem.

Table 1. Computed L_2 error norms with different viscosities for the analytic problem using the Legendre-polynomial finite-element model ($u = 1, v = 1$)

Grid	$\mu = 1.0$	$\mu = 1.0 \times 10^{-1}$	$\mu = 1.0 \times 10^{-2}$
11×11	1.175×10^{-9}	1.217×10^{-9}	4.407×10^{-6}
21×21	1.095×10^{-9}	1.156×10^{-9}	5.885×10^{-8}
31×31	1.174×10^{-9}	1.134×10^{-9}	3.694×10^{-10}
41×41	1.073×10^{-9}	1.112×10^{-9}	2.865×10^{-10}
51×51	1.090×10^{-9}	1.106×10^{-9}	2.671×10^{-10}

Table 2. Computed L_2 error norms with different viscosities for the analytic problem using the characteristic Galerkin finite-element model ($u = 1, v = 1$)

Grid	$\mu = 1.0 \times 10^{-2}$	Rate of convergence	$\mu = 1.0 \times 10^{-3}$	Rate of convergence	$\mu = 1.0 \times 10^{-5}$	Rate of convergence
11×11	1.125×10^{-1}		1.508×10^{-2}		1.575×10^{-4}	
21×21	7.616×10^{-2}	0.563	2.184×10^{-3}	2.787	2.569×10^{-7}	9.259
31×31	6.220×10^{-2}	0.499	4.929×10^{-4}	3.671	6.976×10^{-10}	14.572
41×41	5.483×10^{-2}	0.438	1.455×10^{-4}	4.241	2.966×10^{-12}	18.980
51×51	5.026×10^{-2}	0.389	5.178×10^{-5}	4.630	7.250×10^{-13}	6.314

the characteristic Galerkin finite-element model to problems with higher Peclet numbers. It is also important to note that computational experience tells us that oscillation-free solutions are not found for problems with Peclet numbers higher than 20 using the Legendre-polynomial finite-element model.

For the sake of completeness, we have also investigated the effect of flow angles on the solution quality. To accomplish this goal, we considered another flow

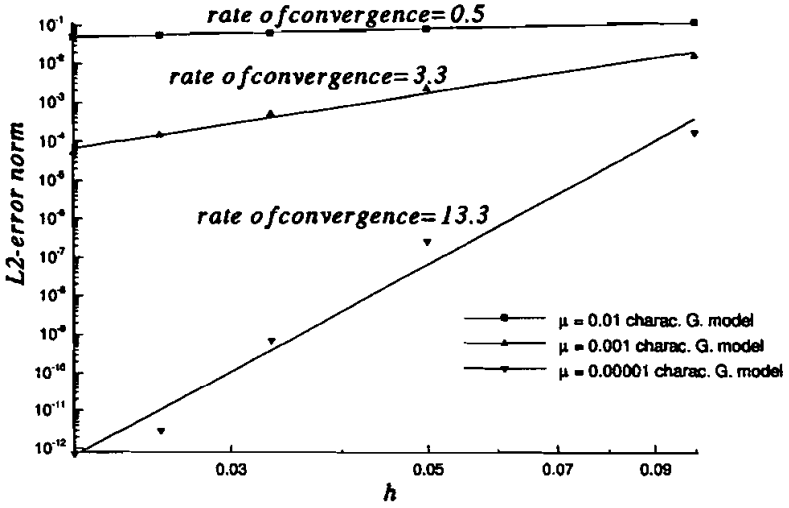

Figure 5. Rates of convergence for the analytic test problem.

Table 3. Computed L_2 error norms for the analytic problem using the Legendre-polynomial finite-element model with different flow directions ($\mu = 0.01$)

Grid	$u = 1, v = 1$	$u = 1, v = 0.5$
11 × 11	4.407×10^{-6}	1.357×10^{-8}
21 × 21	5.885×10^{-8}	8.586×10^{-10}
31 × 31	3.694×10^{-8}	5.534×10^{-10}
41 × 41	2.865×10^{-10}	7.628×10^{-10}
51 × 51	2.671×10^{-10}	5.670×10^{-10}

condition. The case considered is that with constant velocities given by $u = 1$ and $v = 0.5$. Solutions were sought at grids similar to those for the case of ($u = 1, v = 1$). For comparison, we plot the computed error norms for both schemes and flow conditions here in Tables 3 and 4. The value of the investigated viscosity is 0.01. As Tables 3 and 4 reveal, the computed quality using the characteristic Galerkin finite-element model deteriorates as the flow angle moves away from 45°. The shift condition is, in fact, accommodated in the characteristic Galerkin finite-element model. As to the quality of the computed solutions using the Legendre-polynomial finite-element model, it is affected very little. Before considering the next test problem, it is worthwhile to examine in Figure 6 the computed profiles of the passive scalar for both schemes. These profiles are plotted at $y = 0.5$ for different grid resolutions under intermediate Peclet numbers such that monotone solutions can be ensured. As Tables 1 and 2 indicate, the solution accuracy obtained using the Legendre-polynomial finite-element model is much better than that obtained using the characteristic Galerkin finite-element model.

Skew Advection-Diffusion Problem

An even harder problem, configured in Figure 7, follows. This problem, known as the skewed flow transport problem, is featured as having an internal layer and is regarded as a worst-case scenario for any upwinding method. Within a square cavity of unit length, a tilted line passing through a corner point at (0, 0), making a slope of $m = v/u$, divides the unit square into two subdomains. For this study, the y directional component of the velocity remains unchanged with $v = 1$ in the whole domain. Subject to the boundary condition for the working variable, a sharp change in the transport variable is observed across this dividing line.

Table 4. Computed L_2 error norms for the analytic problem using the characteristic Galerkin finite-element model with different flow direction ($\mu = 0.01$)

Grid	$u = 1, v = 1$	$u = 1, v = 0.5$
11 × 11	1.125×10^{-1}	1.401×10^{-1}
21 × 21	7.616×10^{-2}	1.092×10^{-1}
31 × 31	6.220×10^{-2}	9.756×10^{-2}
41 × 41	5.483×10^{-2}	9.139×10^{-2}
41 × 41	5.026×10^{-2}	8.759×10^{-2}

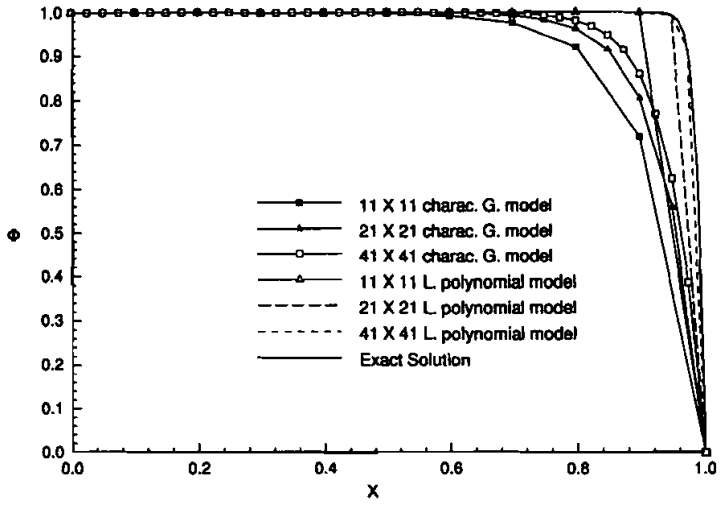

Figure 6. Computed solution profiles at $y = 0.5$ for the analytic test problem for the case of $\mu = 0.01$.

The aim of investigating this case is to demonstrate the effectiveness of the composite monotonic scheme in resolving a high-gradient solution profile in the flow. Since this problem is not amenable to analytic solution, the solution computed at the finest grid resolution of 160×160 is taken as a reference for comparison. This problem is conducted in a unit square that is also covered with uniform grids of different resolutions. Different diffusivities are considered in this study to examine the sensitivity of the proposed scheme to the Peclet numbers. Given that the value of μ is as low as 1.67×10^{-2}, the Peclet numbers still fall within the monotonic region for a grid with 21×21 resolution. We apply the Legendre-polynomial finite-element model. With continuous reduction of the diffusivities, namely, $\mu = 1.0 \times 10^{-3}$ and $\mu = 1.0 \times 10^{-5}$, we use the characteristic Galerkin finite-element model. According to the solution profiles shown in Figure 8, we can capture nonoscillatory high-resolution solutions in the whole

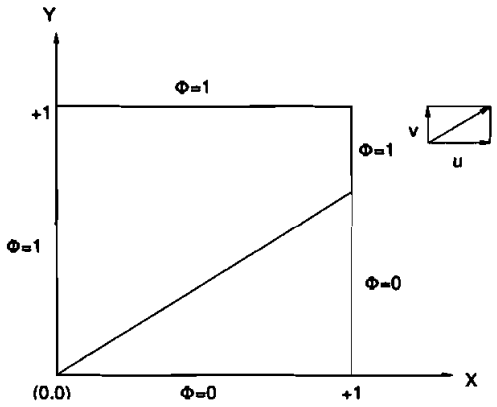

Figure 7. Illustration of the skew advection-diffusion problem.

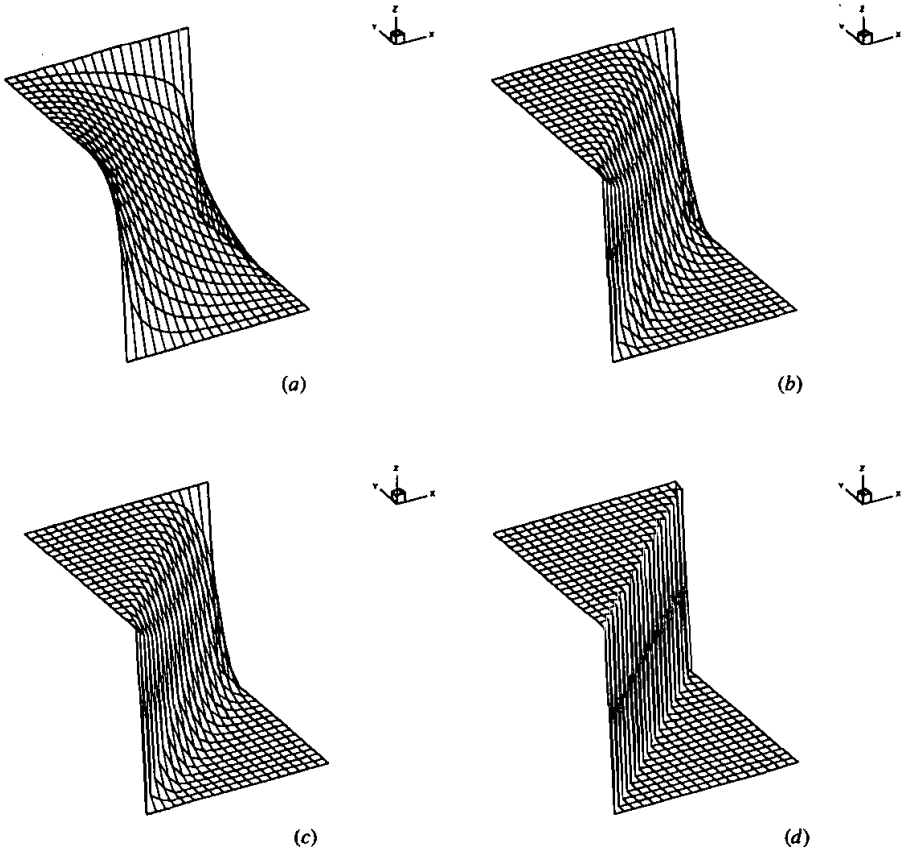

Figure 8. Computed solutions for the skew advection-diffusion problem for the case with 21 × 21 grids: (*a*) $\mu = 0.1$ using the Legendre-polynomial model; (*b*) $\mu = 1.67 \times 10^{-2}$ using the Legendre-polynomial model; (*c*) $\mu = 1.0 \times 10^{-3}$ using the characteristic Galerkin model; (*d*) $\mu = 1.0 \times 10^{-5}$ using the characteristic Galerkin model.

range of Peclet numbers. For clearness, we also plot in Figure 9 the solution profiles at $y = 0.5$ for different grid resolutions. For the sake of completeness, we consider the case with $(u, v) = (0.5, 1)$. As Figure 10 reveals, monotonic solutions are also computable using the Legendre-polynomial finite-element model for cases with larger viscosities while the characteristic Galerkin finite-element model is used for smaller viscosities.

CONCLUDING REMARKS

Two classes of upwind finite-element schemes for discretizing advective fluxes have been selected for use in the present study. The first approach falls into the Petrov-Galerkin context, where both the biased finite-element test space and the basis space are spanned by the Legendre polynomials. The other approach considered here is due to Rice and Schnipke [16]. The underlying idea in formulating the

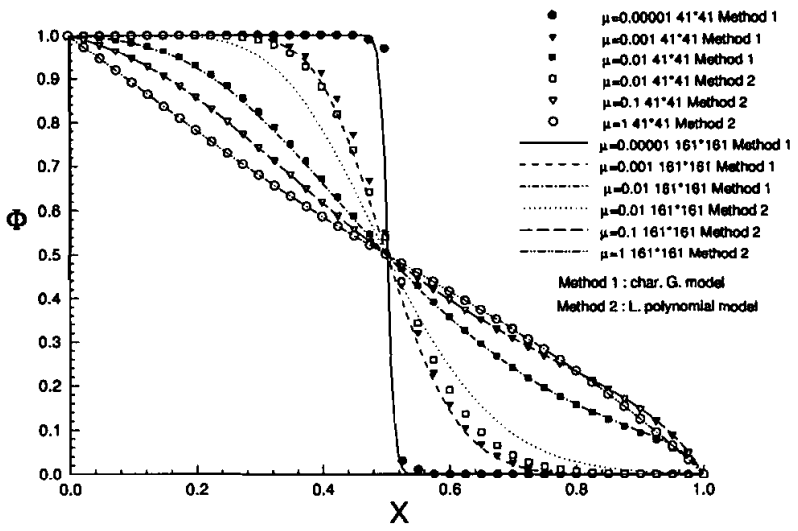

Figure 9. Computed solutions profiles at $y = 0.5$ for the skew advection-diffusion problem for the case of $(u, v) = (1, 1)$ at different viscosities.

upwinding capability is to take the flow characteristics into consideration. This comparison study has addressed solution accuracy as well as solution monotonicity. Both schemes under investigation accommodate monotonic matrices. The underlying theory used to determine whether or not the solution monotonicity can be ensured is based on the discrete-maximum principle. Matrix equations obtained

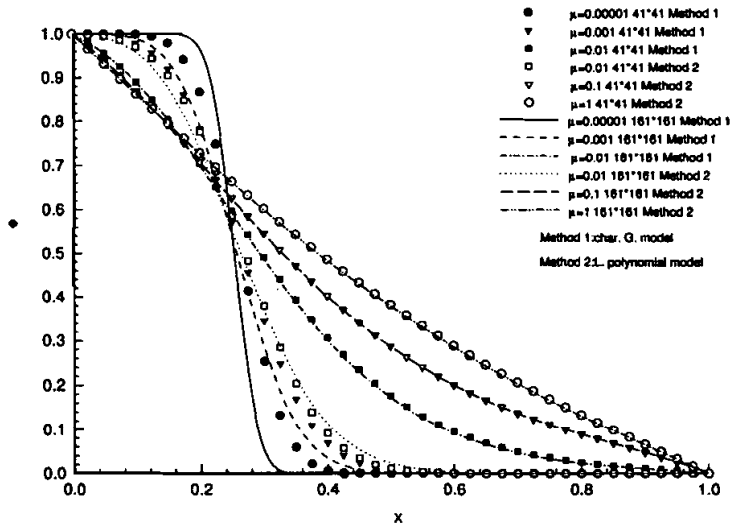

Figure 10. Computed solutions profiles at $y = 0.5$ for the skew advection-diffusion problem for the case of $(u, v) = (0.5, 1)$ at different viscosities.

from two different schemes fall into the monotonic category. Monotonicity can be achieved by choosing the Legendre polynomials to span the test space or by incorporating the flow characteristics into the finite-element formulations. Computational exercises reveal that the Legendre-polynomial finite-element model is most applicable to lower Peclet numbers, while the characteristic Galerkin finite-element model is best suited for higher Peclet numbers. With this fact in mind, we have proposed a hybrid monotonic finite-element model to capture the flow discontinuity for all Peclet numbers.

REFERENCES

1. A. Harten, High Resolution Schemes for Hyperbolic Conservation Law, *J. Comput. Phys.*, vol. 49, pp. 357–393, 1983.
2. J. P. Boris and D. L. Book, Flux Corrected Transport I SHASTA, A Fluid Transport Algorithm That Works, *J. Comput. Phys.*, vol. 11, pp. 38–69, 1973.
3. S. T. Zalesak, Fully Multidimensional Flux-Corrected Transport Algorithm for Fluids, *J. Comput. Phys.*, vol. 31, pp. 335–362, 1979.
4. M. Chapman, FARM-Nonlinear Damping Algorithm for the Continuity Equation, *J. Comput. Phys.*, vol. 44, pp. 84–103, 1981.
5. T. W. H. Sheu, S. M. Lee, K. O. Yang, and B. J. Y. Chiou, A Non-Oscillating Solution Technique for Skew and QUICK-Family Schemes, *Comput. Mech.*, vol. 8, pp. 365–382, 1991.
6. T. W. H. Sheu, P. G. Y. Huang, and M. M. T. Wang, A Discontinuity SUPG Formulation Using Quadratic Elements, in Ch. Hirsch (ed.), *Proc. First European Computational Fluid Dynamics Conf.*, vol. 1, pp. 125–129, Elsevier, Amsterdam, 1992.
7. B. P. Leonard, Simple High-Accuracy Resolution Program of Convective Modeling of Discontinuity, *Int. J. Numer. Meth. Fluids*, vol. 8, pp. 1291–1318, 1988.
8. B. P. Leonard, A. P. Lock, and M. K. MacVean, The NIRVANA Scheme Applied to One-Dimensional Advection, *Int. J. Numer. Meth. Heat Fluid Flow*, vol. 5, pp. 341–377, 1995.
9. B. P. Leonard, A. P. Lock, and M. K. MacVean, Extend Numerical Integration for Genuinely Multidimensional Advective Transport Insuring Conservation, in *Numerical Methods in Laminar and Turbulent Flow '95*, vol. IX, part 1, pp. 1–21, 1995.
10. P. H. Gaskell and A. K. C. Lau, Curvature Compensated Convective Transport: SMART a New Boundedness Preserving Transport Algorithm, *Int. J. Numer. Meth. Fluids*, vol. 8, pp. 617–641, 1988.
11. R. Lönher, K. Morgan, J. Peraire, and M. Vahdati, Finite Element Flux-Corrected Transport (FEM-FCT) for the Euler and Navier-Stokes Equations, *Int. J. Numer. Meth. Fluids*, vol. 7, pp. 1093–1109, 1987.
12. T. W. H. Sheu and C. C. Fang, A Flux Corrected Transport Finite Element Method for Multi-dimensional Gas Dynamics, *Proc. Second European Computational Fluid Dynamics Conference (ECCOMAS)*, pp. 170–175, Elsevier, Amsterdam, 1994.
13. T. W. H. Sheu and C. C. Fang, A High Resolution Finite Element Analysis for Nonlinear Acoustic Wave Propagation, *J. Comput. Acoustics*, vol. 2, pp. 29–51, 1994.
14. T. W. H. Sheu and C. C. Fang, A Numerical Study of Nonlinear Propagation of Disturbances in Two-Dimensions, *J. Comput. Acoustics*, vol. 4, no. 3, pp. 291–319, 1996.
15. S. Spekreijse, Multigrid Solution of Monotone Second-Order Discretizations of Hyperbolic Conservation Laws, *Math. Comput.*, vol. 49, pp. 135–155, 1987.
16. J. G. Rice and R. J. Schnipke, A Monotone Streamline Upwind Finite Element Method for Convection-Dominated Flows, *Comput. Meth. Appl. Mech. Eng.*, vol. 47, pp. 313–327, 1983.

17. T. Meis and U. Marcowitz, Numerical Solution of Partial Differential Equations, in *Applied Mathematical Science*, vol. 32, Springer-Verlag, Berlin, 1981.
18. T. Ikeda, Maximal Principle in Finite Element Models for Convection-Diffusion Phenomena, in *Numerical and Applied Analysis*, vol. 4, North-Holland, Kinokuniya, Amsterdam, Tokyo, 1983.
19. M. Ahue's and M. Telias, Petrov-Galerkin Scheme for the Steady State Convection Diffusion Equation, *Finite Elements in Water Resources* 2/3, 1982.
20. D. L. Hill and E. A. Baskharone, A Monotone Streamline Upwind Method for Quadratic Finite Elements, *Int. J. Numer. Meth. Fluids*, vol. 17, pp. 463–475, 1983.
21. T. W. H. Sheu, M. M. T. Wang, and S. F. Tsai, A Petrov-Galerkin Finite Element Model for Analyzing Incompressible Flows at High Reynolds Numbers, *Int. J. Comput. Fluid Dynamics*, vol. 5, pp. 213–230, 1995.
22. T. W. H. Sheu, S. F. Tsai, and M. M. T. Wang, A Monotone Multidimensional Upwind Finite Element Method for Advection-diffusion Problems, *Int. J. Numer. Heat Transfer, Part B: Fundamentals*, 29:325–344, 1996.
23. T. W. H. Sheu, S. F. Tsai, and M. M. T. Wang, A Monotone Finite Element Method with Test Space of Legendre Polynomials, *Comput. Meth. Appl. Mech. Eng.*, in press.